Journal of Engineering and Applied Sciences 13 (24): 10271-10281, 2018
ISSN: 1816-949X

Effect of Inlet and Outlet Air Terminals Location on the Temperature Distribution and Contaminates Concentration in a Laboratory under Iraqi Climate

[1]Ala'a Abbas Mahdi, [2]Mohammed Wahhab Khadim and [2]Ammar Abdulhussein Mohammed Hassn
[1]Department of Mchanical Engineering, College of Engineering, University of Babylon, Babylon, Iraq
[2]Department of Mechanical Engineering, College of Engineering, University of Kerbala, Kerbala, Iraq

Abstract: Ventilation is the main performance requirement in laboratory design, as it has to guarantee a safe and comfortable indoor environment. Standards and guidelines on laboratory ventilation often impose high ventilation rates increasing the energy need for ventilation. This research focuses on the steady-state distribution of temperature and contaminate concentrations in a real environment which was a function of several factors such as the position of air inlet and exhausts. Different distances between inlet diffuser and exit grill were investigated to determine the optimum distances between inlet diffuser and exit grill. CO_2 is used as an indicator of the concentration of pollutants inside tested room. Room concentration patterns for a laboratory were simulated with Computational Fluid Dynamics (CFD) simulations by using (ANSYS 14) computer programs for various distances. The computational results were validated with design data due to Iraqi cooling code (setup temperature and temperature difference from head to foot level). The numerical results showed that the exhaust grills located near the ceiling resulted in lower pollutant concentrations than the corresponding exhausts near the floor.

Key words: Mixing ventilation indoor air quality, air distribution performance index, numerical model, Iraqi cooling code, foot level

INTRODUCTION

The rate of ventilation airflow has known as the major factor for measuring the quality of indoor air. The air flow rate has been shown to have an impact on respiratory diseases, productivity, air quality and on "sick building syndrome" symptoms (Einberg, 2005). Exposure to chemicals has become a concern for health recently. Most people at risk of chemicals who work in laboratories and thus are more susceptible than others are to various blood diseases such as cancer. The primary purpose of laboratory ventilation is to provide a safe working environment for the experimental staff, so far as possible to avoid long-term work in dangerous air and harm to health. The general reason for setting up air-conditioners system is to keep the temperature and humidity in the room in order that the personnel can work in an appropriate environment to enhance the work efficiency. Some labs submit special requirements for cleanliness and temperature and humidity (Sandru and Ouyang, 2005). Heating, ventilation and air conditioning systems are define as which system capable of providing a comfortable and healthy environment for the occupants. The major factor of poor indoor air quality is because of ineffective ventilation of indoor spaces. After several complaints about indoor air quality problems, the World Health Organization (NIOSH) has conducted more than 500 research on indoor air quality, since, 1971. More than 52% of these investigations believed that the cause of the complaints of the occupants was the lack of ventilation system construction or malfunctioning of these systems (Salisbury 1989; Seitz, 1989). By Khan *et al.* (2006), it was found that the location of the exhaust air grilles when it is in the same wall with the inlet air terminal is better than they locate in two different walls. Nielsen (2009) concluded from research, when applying a mixed or vertical ventilation system to analyze the movement of pollutants by using trace gas that pollutions such as virus and bacteria can decrease when the air velocity increases level within the ventilated space and that these levels of air velocity can be accomplished using these two systems. Xu *et al.* (2009) showed that the increase in ventilation rate does not necessarily reduce the percentage of contaminants in closed areas. If the emission of pollutants is close to the air exit, the concentration of contaminants in the rest of the laboratory may be low. The objective of present work is to investigate a numerical study for an internal combustion

Corresponding Author: Ala'a Abbas Mahdi, Department of Mchanical Engineering, College of Engineering, University of Babylon, Babylon, Iraq

engine laboratory to forecast the thermal comfort and interior airflow by embrace a mixing ventilation system with diverse distances and locations between exhaust air grills and supply air diffusers. The numerical results compared with the standard value due to Iraqi cooling code and ASHRAE standards.

MATERIALS AND METHODS

Theoretical analyses: A laboratory of inner dimensions (14*7*3.75) m with a mixing ventilation system is adopter as a case study tested room as shown in Fig. 1.

All dimensions and power sources from the objects and occupants inside the laboratory are lists in Table 1. The heat transfer through the walls have been calculated

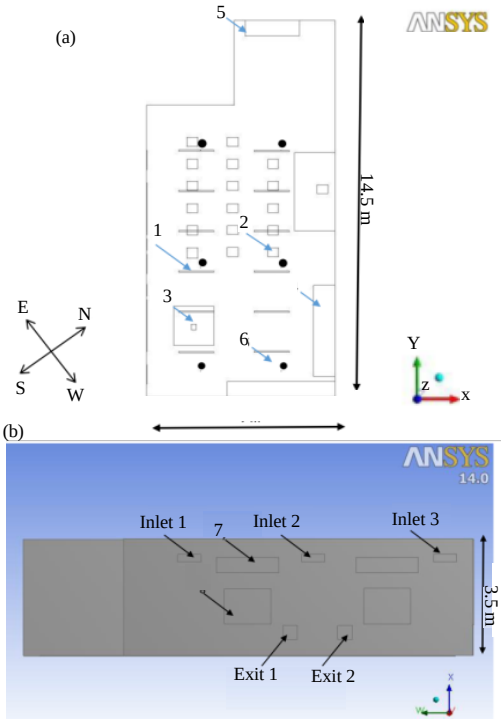

Fig. 1: Sketch of full-scaleinternal combustion engine laboratory

Table 1: Dimensions and powersources for theobjectsand occupants in the laboratory

		Dimensions (m)			
Components	No.	X	Y	Z	Heat-flux (W)
Persons	18	0.40	1.10	0.35	75-per-person
Table	3	0.80	0.75	2.50	0
Supply diffusers	3	0.75	0.25	0.00	-
Exhaust grilles	2	0.46	0.46	0.00	-
Lamps	12	0.05	0.02	1.30	36
Door	1	0.20	1.00	1.50	-
Small window	2	0.00	2.00	0.50	60
Large window	2	0.00	1.05	1.15	212

depending on the Iraqi indoor and outdoor conditions. In Iraqi buildings, the walls mainly formed from multi-materials as (cement, common brick and gypsum) as displayed in Fig. 2.

South-east wall exposed to outside conditions while other room sides are partitions between rooms at same design inside air temperature (24°C Iraqi standard for cooling tables). Six vertical poles (1-6) used, each pole has a height of 2 m and contains five points utilized to gauge the temperature, velocity of air and the concentration of carbon dioxide in the verified room at different levelsas shown in Fig. 3.

Indoor air temperature can be provide by air terminal supply system depending on the total loads of the room occupied. Depending on tables listed in Table 2 shows data that can be used to calculate heat transfer through walls in the present study. From the following steps, the supply air temperature and velocity depend on the overall load.

The first step: Finding the heat transfer from outdoor to indoor by employing Cooling Load Temperature Difference Method (CLTD). Heat transfer through internal walls due to conduction:

$$Q = UA\Delta T \tag{1}$$

$$U = \frac{1}{R_T} \tag{2}$$

$$R_T = \frac{1}{h_i} + \frac{x_1}{k_1} +, ..., + \frac{1}{h_0} + \frac{x_n}{k_n} \tag{3}$$

Heat transfer through external walls (exposed to outside conditions) due to conduction:

$$Q = U * A * CLTD_c \tag{4}$$

$CLTD_C$: Correct-coolingload Temperature Difference. For walls:

$$CLTD_c = (CLTD+LM)*K+ (25.5T_i)+(T_m-29.4)(2.5) \tag{5}$$

For doors and windows:

$$CLTD_c = CLTD+(25.5-T_i)+ (T_m-29.4)(2.6) \tag{6}$$

Table 2: Heat transfer details through walls and window at 30 Jul., 15:00 O'clock in the city of Karbala, Latitude 32.6°

Walls	CLTD	LM	K	SHG	SC	CLF
South East wall	7	-0.5	0.83	-	-	-
Window	8	-	-	508	1	0.53

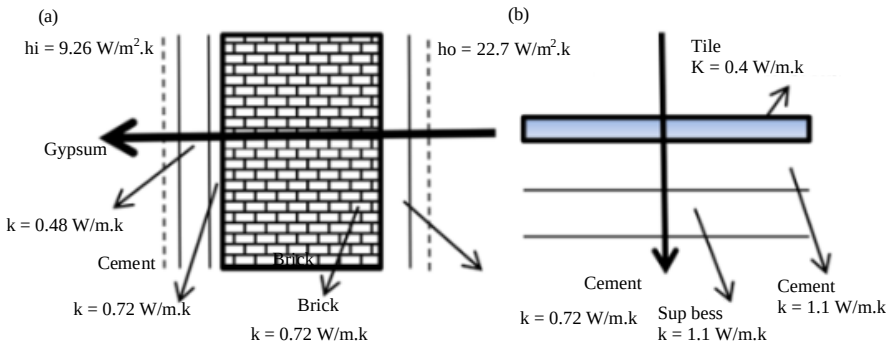

Fig. 2: a) Construction of the wall and b) Construction of the ground

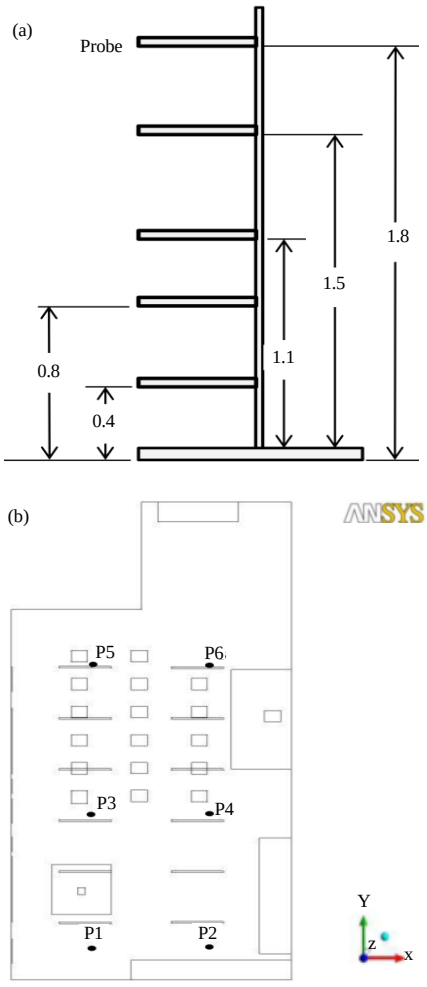

Fig. 3: The measurement poles: a) Schematic diagram and b) Poles locations

Where:

LM = Parameter for month and latitude corrector
T_i = Inside room temperature
T_m = T_0-DR/2
T_m = Outlet design temperature (°C)
T_o = Outlet temperature

Table 3: Valuesofairflowrate, supplytemperaturesand heat transfers

			Heat transfer (W)			
Q-l/(sec)	T_s (°C)	ACH	----------Window------		South East wall	Ground
930	12.6	10	Conduction 1.348	Radiation 269.24	Conduction 1926.53	Conduction 294

The heating load by solar radiation through the window evaluated as:

$$Q_r = A * SC * SHG * CLF \quad (7)$$

The second step: Determine the temperatures of supply air (T_s) and flow rate of air (Chen and Glickman, 2003):

$$Q = \left(0.295q_{oe} + 0.132q_l + 0.185q_{ex}\right) / \left(\rho c_p \Delta T_{hf}\right) \quad (8)$$

$$T_s = T_{sp} - \Delta T_{hf} - \left[\left(A_z . q_t\right) / \left(0.584Q^2 + 1.208A . Q_s\right)\right] \quad (9)$$

$$q_t = q_{oe} + q_l + q_{ex} \quad (10)$$

Then, assume ΔT_{hf} = 3°C (Ashrae, 2001) T_{sp} = 24, T_o = 51°C, the air flow rate values (Q) and temperature of the supply air are calculated and listed in Table 3. Since, the Air Change per Hour (ACH) obtained by:

$$ACH = \left(Q / V_{room}\right) * 3600 \quad (11)$$

CFD mode: Flow supposed to be steady, three-dimensional flow incompressible and sturbulent. Air was assume as a working fluid. The governing equations of motion based on Navier-Stockes conservation equations which are continuity, momentum, energy and species equations (Versteeg and Malalasekera, 1996). The (RNG) k-ε Model used in the CFD simulation program is because of their accuracy and closer to the reality than the other models of turbulent for indoor airflow (Hussein, 2013; Lim *et al*., 2005):

The RNG k-ε Model: The RNG k-ε turbulence model is derived from the instantaneous Navier-Stokes equations by using a mathematical technique called "Renormalization Group" (RNG) method. The RNG k-ε Model is very similar in form to the standard k-ε Model. For incompressible flows, the transport equations for k and ε are as follows:

$$\frac{\partial}{\partial t}(pk)+\frac{\partial}{\partial x_i}(\rho k u_i)=\frac{\partial}{\partial x_j}\left[(\alpha_k\mu_{eff})\frac{\partial k}{\partial x_j}\right]+G_k+$$
$$G_b-\rho\varepsilon+S_k\frac{\partial}{\partial t}(\rho\varepsilon)+\frac{\partial}{\partial x_i}(\rho\varepsilon u_i)\ \frac{\partial}{\partial x_j}\left[(\alpha_k\mu_{eff})\frac{\partial \varepsilon}{\partial x_j}\right]+ \quad (12)$$
$$C_{1\varepsilon}\frac{k}{\varepsilon}(G_k+C_{3\varepsilon}G_b)-C_{2\varepsilon}\rho\frac{\varepsilon^2}{k}-R_\varepsilon+S_\varepsilon$$

where, G_k and G_b terms in the above equations represent the generation of turbulence kinetic energy due to the mean velocity gradients and due to Buoyancy, respectively, they are calculated using Eq. 7 and 8. The quantities of α_k and $\alpha_{\hat{a}}$ are the inverse effective Prandtl-numbers for k and ε, respectively S_k and S_ε are the source terms for k and ε, respectively:

$$G_k=-\overline{\rho u_i' u_j'}\frac{\partial u_j}{\partial x_i}=\mu_t\left(\frac{\partial u_j}{\partial x_j}+\frac{\partial u_j}{\partial x_i}\right)\frac{\partial u_j}{\partial x_i} \quad (13)$$

And G_b represents the production of turbulent kinetic energy due to Buoyancy:

$$G_b=\beta g_i\frac{u_t}{\sigma_t}\frac{\partial T}{\partial x_i} \quad (14)$$

Where:

g_i = The component of the gravitational vector in i-direction

β = The thermal expansion coefficient

Defined as:

$$\beta=-\frac{1}{\rho}\left(\frac{\partial \rho}{\partial T}\right)_P \quad (15)$$

For an ideal gas, Eq. 8 reduces to:

$$G_b=-g_i\frac{\mu_t}{\rho\sigma_t}\frac{\partial \rho}{\partial x_i} \quad (16)$$

The turbulent (Eddy) viscosity μt is obtaine by combining k and ε as follows:

$$\mu_t=\rho C_\mu\frac{k^2}{\varepsilon} \quad (17)$$

C_μ, $C_{1\varepsilon}$, $C_{2\varepsilon}$ and $C_{3\varepsilon}$ are model coefficients constants and $C_\mu=0.09$, $C_{1\varepsilon}=1.44$ $C_{2\varepsilon}=1.92$ $C3_\varepsilon$ is determined from Eq. 18:

$$C_{3\varepsilon}=\tanh\left|\frac{v}{u}\right| \quad (18)$$

Where:

v = The component of the flow velocity parallel to the gravitational vector

u = The component of the flow velocity perpendicular to the gravitational vector

The scale elimination procedure in RNG theory results in a differential the equation for turbulent viscosity:

$$d\left(\frac{\rho^2 k}{\sqrt{\varepsilon\mu}}\right)=1.72\frac{\hat{\nu}}{\sqrt{\hat{\nu}^3-1+C_\nu}}d\hat{\nu} \quad (19)$$

where, $\hat{\nu}=\mu_{eff}/\mu$, $C_\nu\approx 100$. By integrating Eq. 17, an accurate description of how the effective turbulence transport varies with the effective Reynolds number (or Eddy scale) can obtained which allows the model to better handle low-Reynolds number and near-wall flows. The inverse effective Brandt numbers $\alpha_{k.}$ and α_ε are compute utilize the followings formula derived-s from the RNG theory:

$$\left|\frac{\alpha-1.3929}{\alpha_0-1.3929}\right|^{0.6321}\left|\frac{\alpha+2.3929}{\alpha_0-2.3929}\right|^{0.6321}=\frac{\mu_{mol}}{\mu_{eff}} \quad (20)$$

where, $\alpha=1/\sigma k=1/\sigma\varepsilon=1/\sigma t$ and $\alpha 0=1.0$. In the high-Reynolds-number limit ($\mu/\mu_{eff}<<1$), $\alpha k=\alpha\varepsilon\approx 1.393$ that means the effective Brandt numbers for k and ε are about 0.7178:

$$R_\varepsilon=\frac{C_\mu\rho\eta^3\left(1-\frac{\eta}{\eta_0}\right)}{1+\beta\eta^3}\frac{\varepsilon^2}{k} \quad (21)$$

Where:

$$\eta\equiv\frac{sk}{\varepsilon},\ \eta_0=4.38 \text{ and } \beta=0.012$$

The ε equation can be rewrite as:

$$\frac{\partial}{\partial t}(\rho\varepsilon)+\frac{\partial}{\partial x_i}(\rho\varepsilon U_i)=\frac{\partial}{\partial x_j}\left[(\alpha_\varepsilon\sigma_\varepsilon\mu_{eff})\frac{\partial \varepsilon}{\partial x_j}\right]+$$
$$C_{1\varepsilon}\frac{k}{\varepsilon}(G_k+C_{3\varepsilon}G_b)-C_{2\varepsilon}^*\rho\frac{\varepsilon^2}{k}+S_\varepsilon$$

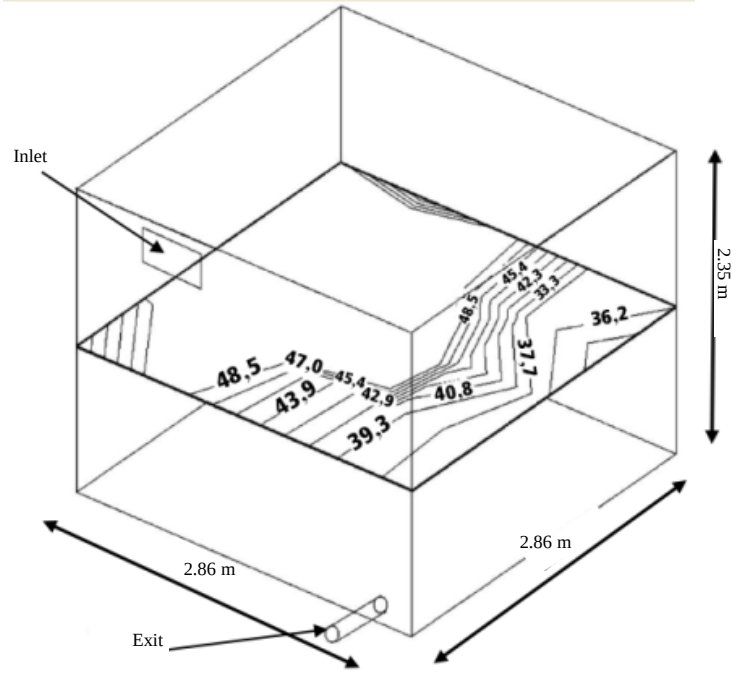

Fig. 4: Schematic diagram of the validation case (Khan *et al*., 2006)

where, $C^{*}_{2\varepsilon}$ is given by:

$$C^{*}_{2\varepsilon} = C_{2\varepsilon} + \frac{C_{\mu}\eta^{3}\left(1-\frac{\eta}{\eta_{0}}\right)}{1+\beta\eta^{3}}$$

In areas where, $\eta<\eta_{0}$, the R term makes a positive scontribution and $C^{*}_{2\varepsilon}$ becomes greater than $C_{2\varepsilon}$ In the logarithmic layer for instance it can bedisplayed that $\eta \approx 3.0$, giving $C^{*}_{2\varepsilon}\approx 2$ which is near in magnitude to its value inthe standard k-ε Model (1.92). As a result for weakly to moderately strainedflows, the R1N-G Model tends to gives results largely comparable to the standard k-ε Model. In sections of great strain rate ($\eta>\eta_{0}$), however, the R term makesa negative contribution, making the value $C^{*}_{2\varepsilon}$ of less than $C_{2\varepsilon}$ In comparison with the standard k-ε Model, the smaller destruction of ε augments ε, decreasing k and eventually the effective viscosity. The model constants in Eq. 20 are the following values: $C_{1\varepsilon} = 1.42$ and $C_{2\varepsilon} = 1.68$, the coefficient $C_{3\varepsilon}$ is determined by Eq. 16.

Numerical model validation: It was necessary to validate fluent software with another experimental study. The validation isdowning by comparing the RNG k-ε Model results with experimental data obtained in a tested room with a wall supply mixing ventilation system. A room of (2.86×2.86×2.35) m was construct with an insulated interior surface. A rectangular air inlet 0.39×0.24 m was existing

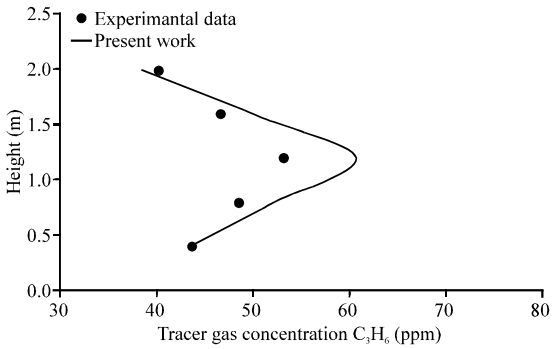

Fig. 5: Validate the RNG K-ε turbulent model with another experimental study (Khan *et al*., 2006)

at one upper-corner and a circular 0.1 m diameter exhaust air grille was situate at the diagonally opposite corner of the inlet air grille on the same wall of the room as shown in Fig. 4. A constant flow of the tracer gas (99.5% propylene) continuously released through a 0.1 m screened opening in the top of a 1-m high pedestal locatedat the center of the room (Khan *et al*., 2006). The comparison depends on the contaminate concentration resulted which listed in Table 1 by Khan *et al.* (2006). The comparison gives a good agreement between the empirical and numericaldata obtained by the RNG k-ε turbulent model as shown in Fig. 5. The average error between the experimental and numerical values calculated is 6.7 %.

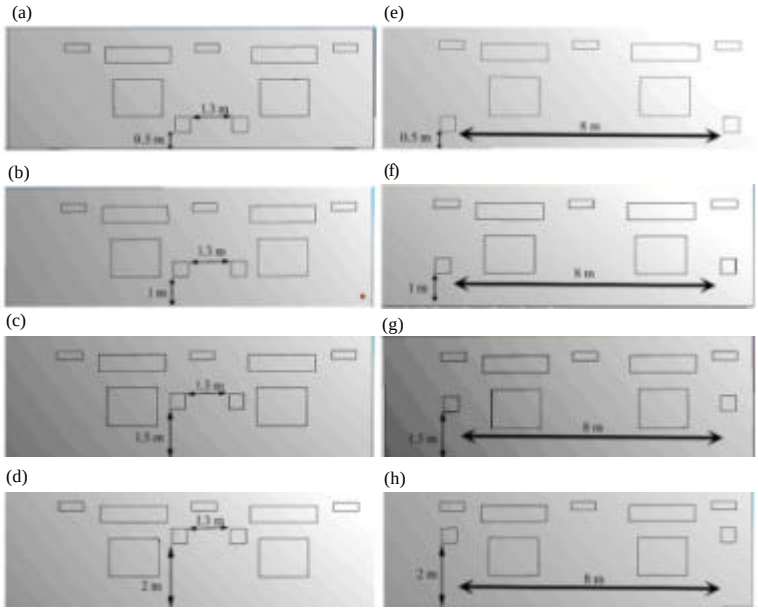

Fig. 6: Case studies adopted in present work: a) Case-1; b) Case-2; c) Case-3; d) Case-4; e) Case-5; f) Case-6; g) Case-7 and h) Case-8

Boundary conditions and numerical solution: The simulation of air flow in a room by CFD be contingent on scorrect description of the boundary conditions by the employer. The supply temperature and heat transfers on the floor, sidewalls and window are calculated and listed in Table 3 to use as boundary conditions for the walls and heated objects in CFD simulations. The carbon dioxide is present in the atmospheric air with concentration at the typical value of 350 ppm (Ashrae, 2001). In the buildings, people are the main sources of the carbon dioxide. Exhaled air contains 4-5% of carbon dioxide. This amount depends on the activity level and the size of the occupants (Versteeg and Malalasekera, 1996; Awbi, 2003). Increase of the carbon dioxide concentration in the room depends on the source strength and the amount of the fresh air entering the space that dilutes the carbon dioxide concentration. The CO_2 concentration levels that occur indoors are harmless and not perceived by humans but they are a good indicator of other bioeffuents from people perceive (Liu *et al*., 2010). Many standards are defne as acceptable level for the carbon dioxide concentration to keepcomfort criteria of the indoor air quality. ASHRAE Standard 62 states that comfort criteria are satisfied if the ventilation rate is enough to keep carbon dioxide level under 1000 ppm (Ashrae, 2001). This is the commonly referenced guideline value for carbon dioxide concentration in the literature (Zhou and Kim, 2010; Santamouris *et al*., 2008; Griffiths and Eftekhari, 2008; ASTM D6245-07, 2007; Persily, 1997). Velocity inlet boundary conditions for both contaminate source inlet air were assume constant and the flow was normal to inlet study. The feature of taking the density of both constituents to be equal and constant is the possibility of making utilize of the Boussinesq approximation to model buoyancy effects. The function of the wall was employ in standard FLUENT (smooth, no slip and no diffusive flux of the species). For discretization were chose the body force weighted scheme for pressure, the simple C scheme for pressure velocity coupling, the second order upwind cheme for momentum, turbulence and species (Aglan, 2003). Presupposed the under relaxation factors in this research when the residuals less than or equal to 10^{-6} for energy and for all scalars $\leq 10^{-3}$.

The cases studies: To compare the indoor particle concentration and deposition, a full scale room with three inlet diffusers and two exist grilles are used. This study applied a different distances between inlet and exit air grilles with eight cases. The height from the ground 0.5 m for case-1 and -5, 1 m for case-2 and -6, 1.5 m for case-3 and -7, 2 m for case-4 and -8. The distance between the two exhaust air grille 1.3 m for cases 1-4 and 8 m for cases 5-8 as shown in Fig. 6.

Mesh generation: The major tasks in pre-processing is to defines the geometry of the computational domain and designates the cellsor element son which the fluid flow equations are solved which known asdomain

Table 4: Skewness ranges and cell quality

Value of skewness	Cell quality
0	Degenerate
<0.02	Bad (sliver)
0.25-0.02	Poor
0.5-0.025	Fair
0.75-0.5	Good
0.75-1	Execellent
1	Equilateral

Table 5: Values of skewness for cases studied

Case study	Value of skewness
1	0.891
2	0.892
3	0.870
4	0.862
5	0.888
6	0.859
7	0.891
8	0.896

Table 6: Values of orthogonal quality for cases studied

Case study	Value of orthogonal quality
1	0.9961
2	0.9963
3	0.9968
4	0.9968
5	0.9969
6	0.9962
7	0.9966
8	0.9961

discretization. The gridhas a great influences on the convergence rate, solution accuracy and computing time. Inadequate grid gives poor predictions while a dense grid demands high computer resources. Skewness is one of the primary quality measures for a mesh. Skewness determines how close to ideal (i.e., equilateral or equiangular) a face or cell is a Table 4.

Table 5 shows skewness for cases studied. The quality of the mesh plays animportant roles in the accuracy and stability of the numeral computation. Regardless of the kind of mesh utilized in the domain, checking the quality of mesh is essential. One important indicator of mesh quality that ANSYS Fluent allows checking is a quantity referred to as the orthogonal quality and the range for orthogonal quality is 0-1 where a value of 0 is worst and a value of 1 is best. Table 6 shown orthogonal quality for cases studied. Figure 7 show part of the meshed model for case-1 and 2, respectively.

The parameters of indoor air quality: For the purpose of maintaining good thermal comfort and indoor air quality by designed the ventilation systems and operated. Based on a number of indicators by which the ventilation system was can be assessed, the efficiency is one of these indicators to achieve these objectives. To calculate the capacity of the ventilation system to remove pollutants and heat generated within the ventilated space through

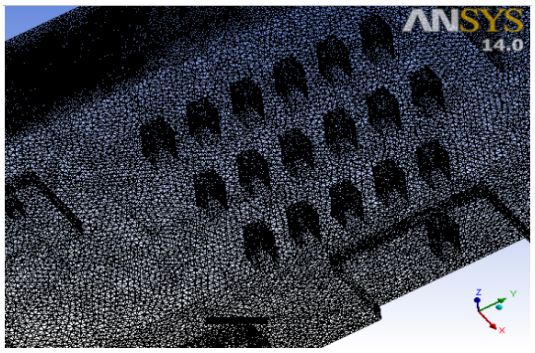

Fig. 7: Part from mesh model for case-1 as a sample

the effectiveness of the removal of the pollutant (ε_c) and the effectiveness of heat removal (ε_t) as expressed (Awbi, 2003):

$$\varepsilon_t = \frac{T_0 - T_i}{T_m - T_i} \quad (22)$$

$$\varepsilon_c = \frac{C_0 - C_i}{C_m - C_i} \quad (23)$$

In Eq. 22 and 23, T is the Temperature of air (°C), C is the contaminate concentration in part per million (ppm), subscripts "o" denote outlet, "i" denote inlet and m denote mean values in the occupied zone.

Air Distribution Performance Index (ADPI): ADPI is used as a measure to evaluate the performance of an air distribution system within a room/zone. Among the several evaluation methods used to design air distribution systems based on flow rate, sound data and comfort criteria, the ADPI selection method is quite commonly used. This parameter is important in describing the air diffusion performance of the publisher in the air-conditioned area. The Effective Draft Temperature (EDT) is acquainted. Ventilation performance index (ADPI) is calculated by the number of measured points in the occupied area and is a percentage. The percentage is extracted by an account of Effective Draft Temperature (EDT) within the limit (>-1.7 and <1.1°C) divided by the measured total number of points. If the ventilation performance index between 60-69, it is not good, then if it between 70-79, it is acceptable and if it is 80 or more, it is good (Awbi, 2003):

$$EDT = (T_x - T_r) - 8(V_x - 0.15) \quad (24)$$

Where:

V_x = The local Velocity and the maximum air velocity was taken as 0.35 (m/sec)
T_x = The local Temperature (°C)
T_r = The room Temperature (°C)

RESULTS AND DISCUSSION

Numerical simulations were conduct to analyze the temperature and CO_2 concentration distributions with the change the space between exhaust grilles and air supply diffusers location. The simulated results were compared with design data (setup temperature and temperature difference from head to foot level) to validate the CFD Model.

Temperature distribution: Figure 8 shows the air temperature distribution in each poles for the 8 cases where it appears that the distribution is approximate in most areas of the 8 cases except remote areas where the rise in temperature with poles (3, 5 and 6) for the 8 cases. The temperatures in the case-4 reaching to (21.2°C), reaching to (21.1°C) for case-6 and reach to (21.1°C) for case-8 near the South East wall in the lower areas, this rise in temperature was due to the position of this poles between the source of heat (persons) in addition to the situation close to the window. While the temperatures fallen with other cases in same region, reach to maximum value (19.1°C) for case-7 as shown in Fig. 8.

Average temperatures throughout for all room was (20.73°C) for the first case, (21.147°C) for second case, (20.17°C) for third case (20.85°C) for forth case (20.77°C) for fifth case (21.163°C) for sixth case (19.4°C) for 7 case and (22.17°C) for 8 case. This leads to raising in the efficiency of removing thermal and increase the air performance distribution index as stipulated in on the other hand the difference in the temperature from head to foot level was not large. The air temperature changes for the above cases between the head to foot level of a sedentary occupant are <3 K as stipulated in ASHRAE. Figure 9 discussed the distribution of air temperature contours for the eight cases at occupied zone. For all cases the relatively cold air which it temperature is 18°C falling from the ceiling diffusers,

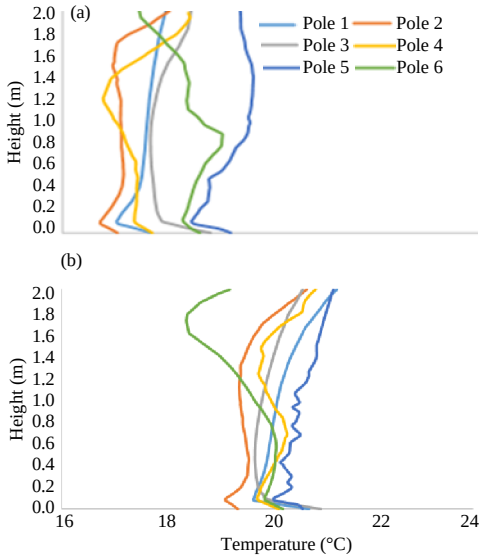

Fig. 8: Vertical air temperature profile at measuring poles for the location of exhaust air grilles; a) z (1.5m) and b) z (2 m) and distances (8 m) between the exhaust air grilles

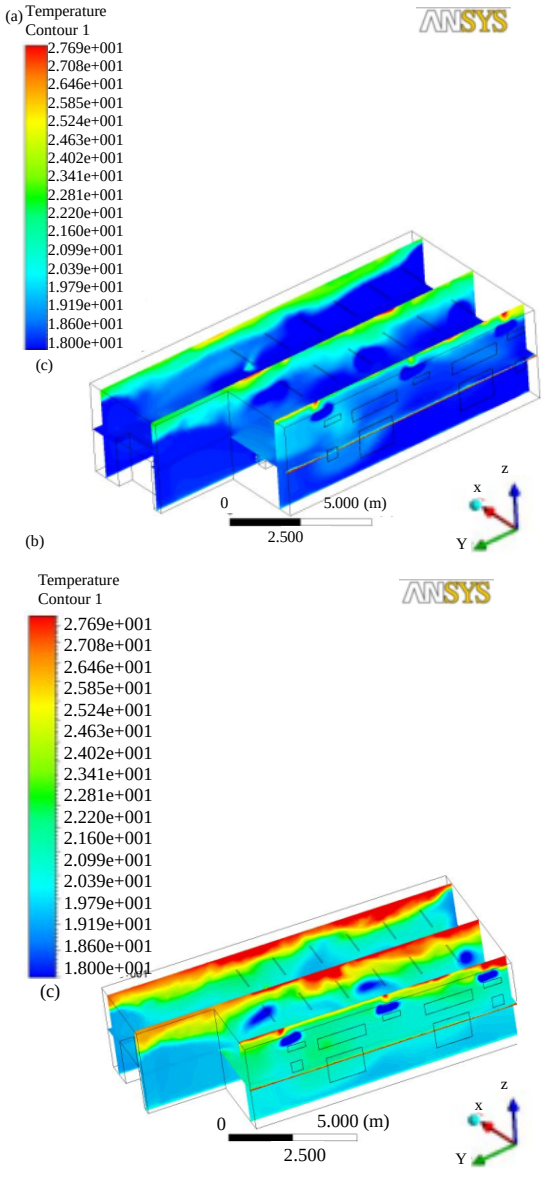

Fig. 9: Distribution of temperature measured in the occupied zone for the location of exhaust air grilles: a) z (1.5 m) and b) z (2 m) and distances (8 m) between the exhaust air grilles

Table 7 : Summary of different result of mixing ventilation method used in this simulation

	Distance (1.3 m)				Distance (8 m)			
Parameters	Case-1 high (0.5 m)	Case-2 high (Lm)	Case-3 high (1.5 m)	Case-4 high (2 m)	Case-5 high (0.5 m)	Case-6 high (Lm)	Case-7 high (1.5 m)	Case-8 high (2 m)
Heat removal effectiveness (εt)	0.891	1.121	1.392	1.3516	1.041	1.121	1.498	1.294
Contaminate removal effectiveness (εc)	0.820	0.819	0.936	0.9710	0.819	0.840	0.889	0.864
APDI	0.810	0.72	0.430	0.4900	0.620	0.670	0.830	0.820
ΔT (K)	0.573	0.57	0.130	0.6115	0.520	0.721	0.484	0.766

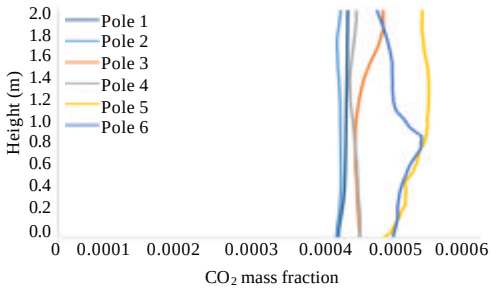

Fig. 10: Vertical contaminate concentrations profile at six measuring poles for the location of exhaust air grilles, z (1.5 m) and distances (8 m) between the exhaust air grilles

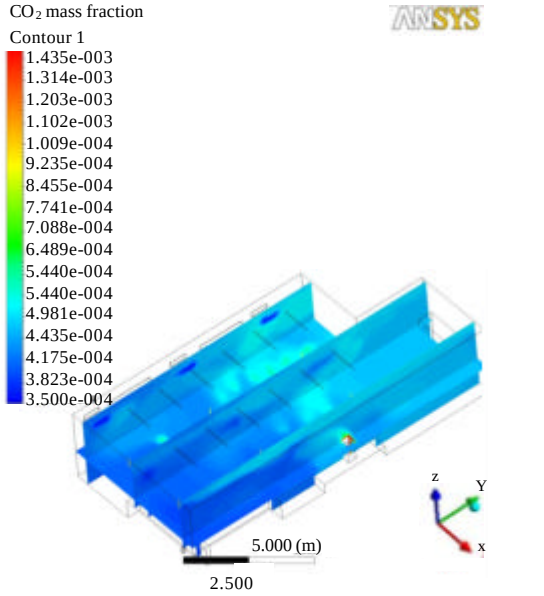

Fig. 11: Distribution of contaminant concentrations in the occupied zone for the location of exhaust air grilles, z (1.5 m) and distances (8 m) between the exhaust air grilles

sprays down to the floor driving by its initial momentum as well as difference in the density. Regular distribution of temperature which appears in the eight cases, leads to increase the thermal efficiency as shown in Table 7.

Where the range of the temperature of medium region is (18-21°C) in the space of activity the occupants (occupied zone) while the temperature reaching to 28°C in the south-east wall due to high external temperatures of this wall compared with the other walls. Exhausts located in the level of breathing always better than their respective exhausts on the other levels, for example, case-3 and -7 are better than other cases. This is because when the exhausts level same as breathing level, the residence time for the ventilation air is small, also, it gets less chance to be mixing with the room air to carry it out of the tested room.

CO_2 concentration distribution: Figure 10 explained the concentration of CO_2 for each poles into 8 cases. The highest ratio of contaminate concentration was recorded for polse 5 and 6 at the concentration (550 ppm) because of its proximity to the source of pollution and large distance from supply air terminal fresh air does not reach to remote areas. Liu *et al*. (2010) show the same result in the corner of the room is a high concentration of contaminants. In all cases the contaminate decreasing in the whole room for the same reason with the temperature distribution while case-3 and -7 was the better than the other cases due to a decrease in the concentration of contaminants for their closeness to the supply air terminal.

High velocity removing more contaminate of the tested room, Zhou and Kim (2010) notes that high velocity of the airflow allows a better removal of contaminate comparison with the other case. In general, exhaust air grilles locations near the source of pollution are better than the far exhausts from pollution, this is because thepath of pollutionis small from inlet to exit, for example, case-3 and -7 is better than the other cases. Figure 11 represented the concentration of the CO_2 in breathing zone at plane z = 1.5 m above the floor, 350 ppm from CO_2 in the ambient. The source of CO_2 in the indoor from the engine and occupants, people are also, a source of heat. The heat produces updraft clouds that can bring the CO_2 to the upperzone. Concentration of most of the place is

about (481) ppm for case-1 and for case-2 and for case-3 while about (423) ppm for case-3 and for case-4 while about (451) ppm for case-6 and (230) ppm for case-7 and -8, this can maintain a better IAQ, especially for breathing zone and increasing pollution efficiency as shown in Table 7.

CONCLUSION

Exhaustive computational investigation was performed tostudy physical factors thataffects distribution of temperature and contaminates concentration in a ventilated internal combustion laboratory under Iraqi climate. The following conclusions were obtain from this study.

The exhaust airgrilles location is very important to take into account to reach human comfort and healthy conditions where higher heat and contaminate removal effectiveness efficiency obtained when the exhausts located near the level of breathing zone than the location far from the breathing zone which was due to short circuiting of fresh inlet air.

The investigation found that if used more exhaust air grilles the distances between them effect on indoor air quality parameters, far distances better that the near distances due to the short path between the contaminant source and the exhaust.

REFERENCES

ASTM D6245-07, 2007. Standard Guide for Using Indoor Carbon Dioxide Concentration to Evaluate Indoor Air Quality and Ventilation. ASTM International, West Conshohocken, Pennsylvania,.

Aglan, H.A., 2003. Predictive model for CO_2 generation and decay in building envelopes. J. Appl. Phys., 93: 1287-1290.

Ashrae, 2001. ASHRAE Standard 62-2001-Ventilation for acceptable indoor air quality. Atlanta: American Society of Heating, Refrigerating and Air-Conditioning Engineers.http://www.bcin.ca/Interface/ openbcin.cgi?submit =submit &Chinkey =234641

Awbi, H.B., 2003. Ventilation of Buildings. 2nd Edn., Spon Press, London, ISBN: 0415270553.

Chen, Q. and L. Glickman, 2003. System Performance Evaluation and Design Guidelines for Displacement Ventilation. American Society of Heating, Refrigerating and Air-Conditioning Engineers (ASHRAE), Atlanta, Georgia,.

Einberg, G., 2005. Air diffusion and solid contaminant behaviour in room ventilation: A CFD based integrated approach. Ph.D Thesis, Royal Institute of Technology, Stockholm, Sweden.

Griffiths, M. and M. Eftekhari, 2008. Control of CO_2 in a naturally ventilated classroom. Energy Build., 40: 556-560.

Hussein, H.M.A., 2013. A theoretical study of a cold air distribution system with different supply patterns. Ph.D Thesis, University of Technology Iraq, Baghdad, Iraq.

Khan, J.A., C.E. Feigley, E. Lee, M.R. Ahmed and S. Tamanna, 2006. Effects of inlet and exhaust locations and emitted gas density on indoor air contaminant concentrations. Build. Environ., 41: 851-863.

Lim, S.C.J., A. Husain and B.T. Tee, 2005. Simulation of airflow in lecture rooms. Proceedings of the 2005 International Conference on AEESAP, June 7-8, 2005, University of Malaya Centre for Continuing Education, Kuala Lumpur, Malaysia, pp: 1-6.

Liu, Z., A. Li, L. Tao and X. Jiao, 2010. Correlation between indoor air distribution and pollutants in natural ventilation. Proceedings of the 4th International Conference on Bioinformatics and Biomedical Engineering (iCBBE'10), June 18-20, 2010, IEEE, Chengdu, China, ISBN:978-1-4244-4712-1, pp: 1-4.

Nielsen, P.V., 2009. Control of airborne infectious diseases in ventilated spaces. J. Royal Soc. Interface, 6: S747-S755.

Persily, A.K., 1997. Evaluating building IAQ and ventilation with indoor carbon dioxide. Trans. Am. Soc. Heat. Refrigerating Air Conditioning Eng., 103: 193-204.

Salisbury, S.A., 1989. Evaluating building ventilation for indoor air quality investigations. Proceedings of the 1989 International Symposium on the Practitioner's Approach to Indoor Air Quality Investigations, May 23, 1989, American Industrial Hygiene Association, Fairfax, Virginia, pp: 87-98.

Sandru, E. and X. Ouyang, 2005. Planning and designing laboratory ventilation systems for the safety of the users and protection of the environment. Proceedings of the 10th International Conference on Indoor Air Quality and Climate-Indoor Air Vol. 4, September 4-9, 2005, United States Environmental Protection Agency, Beijing, China, pp: 3217-3222.

Santamouris, M., A. Synnefa, M. Asssimakopoulos, I. Livada and K. Pavlou *et al*., 2008. Experimental investigation of the air flow and indoor carbon dioxide concentration in classrooms with intermittent natural ventilation. Energy Build., 40: 1833-1843.

Seitz, T.A., 1989. NIOSH Indoor Air Quality Investigations 1971-1988. In: Proceedings of the Indoor Air Quality: The Practitioner's Approach to Indoor Air Quality Investigations, Weedes, D.M. and R.B. Gammage (Eds.). American Industrial Hygiene Association, Fairfax, Virginia, pp: 163-171.

Versteeg, H.K. and W. Malalasekera, 1996. An Introduction to Computational Fluid Dynamics: The Finite Volume Method. Longman Group UK Ltd., Harlow, England, UK.,.

Xu, Y., X. Yang, C. Yang and J. Srebric, 2009. Contaminant dispersion with personal displacement ventilation, Part I: Base case study. Build. Environ., 44: 2121-2128.

Zhou, J. and C.N. Kim, 2010. Numerical investigation of indoor CO2 concentration distribution in an apartment. Indoor Built Environ., 20: 91-100.